Environmental Science & Technology

pubs.acs.org/est

Article

Bacterial Emission Factors: A Foundation for the Terrestrial-Atmospheric Modeling of Bacteria Aerosolized by Wildland Fires

Leda N. Kobziar,* Phinehas Lampman, Ali Tohidi, Adam K. Kochanski, Antonio Cervantes, Andrew T. Hudak, Ryan McCarley, Brian Gullett, Johanna Aurell, Rachel Moore, David C. Vuono, Brent C. Christner, Adam C. Watts, James Cronan, and Roger Ottmar

Cite This: *Environ. Sci. Technol.* 2024, 58, 2413−2422

Read Online

ACCESS | Metrics & More | Article Recommendations | Supporting Information

ABSTRACT: Wildland fire is a major global driver in the exchange of aerosols between terrestrial environments and the atmosphere. This exchange is commonly quantified using emission factors or the mass of a pollutant emitted per mass of fuel burned. However, emission factors for microbes aerosolized by fire have yet to be determined. Using bacterial cell concentrations collected on unmanned aircraft systems over forest fires in Utah, USA, we determine bacterial emission factors (BEFs) for the first time. We estimate that 1.39×10^{10} and 7.68×10^{11} microbes are emitted for each Mg of biomass consumed in fires burning thinning residues and intact forests, respectively. These emissions exceed estimates of background bacterial emissions in other studies by 3−4 orders of magnitude. For the ∼2631 ha of similar forests in the Fishlake National Forest that burn each year on average, an estimated 1.35×10^{17} cells or 8.1 kg of bacterial biomass were emitted. BEFs were then used to parametrize a computationally scalable particle transport model that predicted over 99% of the emitted cells were transported beyond the 17.25 x 17.25 km model domain. BEFs can be used to expand understanding of global wildfire microbial emissions and their potential consequences to ecosystems, the atmosphere, and humans.

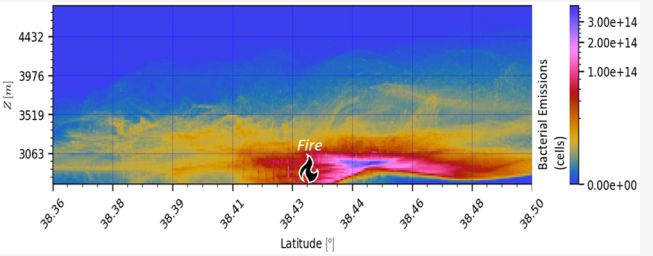

KEYWORDS: *pyroaerobiology, bioaerosol, smoke, aerosol, LIDAR, wildfire, atmospheric transport model, emission*

INTRODUCTION

Microorganisms are aerosolized and transported by winds and wind-generating atmospheric disturbances such as hurricanes and dust storms.[1,2] Recent research has revealed that wildland fires (i.e., wildfires and prescribed fires) are among the mechanisms that aerosolize microbes from terrestrial sources into the atmosphere;[3−6] however, little is known about the scale of these emissions or the distances over which they are transported. Biomass burning is responsible for the global emission of more than ∼2 Pg carbon each year,[7] and viable microbes are a ubiquitous component of biomass fuels burned in wildland fires (i.e., vegetation and soils). Studies of both low- and high-intensity burns in US forests have shown that aerosolized concentrations of microbes in proximity to wildland fires (i.e., within 150 m) are 1−2 orders of magnitude higher than background concentrations.[3,4] The microbial assemblages associated with the smoke are dominated by bacteria and fungi, with the majority of cells inferred to be viable.[3] This suggests that after aerosolization, species capable of surviving atmospheric transport could become established and potentially affect the environments (or hosts) in which they are deposited or inhaled.

Nonbiological wildland fire emissions inventories and transport have been projected using a variety of observational (e.g., satellite-derived), experimental, and modeling approaches. Most fire emission models use emission factors (EFs) that describe the mass of aerosol product per mass of biomass fuel consumed.[8−14] EFs have been quantified for 276 known wildland fire aerosols, including greenhouse gases, volatile organic compounds, polycyclic aromatic hydrocarbons, and carbon in its various forms.[11] EFs are distinguished by fire phase (e.g., smoldering vs flaming), fuel source, and measurement approach[11] and are broadly utilized in smoke models to predict the emission and transport of aerosols.[12,13,15] To model the transport of microbial emissions from wildland fires, EFs specific to the microbial content in smoke are needed. The utility of such emission factors extends from pathogen transport[16−18] to understanding the potential ecological impacts of microbial dispersal on biodiversity,[19] ecosystem

Received: July 11, 2023
Revised: December 31, 2023
Accepted: January 2, 2024
Published: January 24, 2024

function,[20] and atmospheric processes like cloud or ice nucleation.[4,21]

A methodology for determining microbial emission factors has not been established, but the principles upon which existing EFs have been determined can be applied as a first approach to enable validation testing during subsequent fires. EFs are often calculated using the carbon mass balance method,[22] whereby the composite mass concentration of carbon in gaseous and solid form in smoke is assumed to represent approximately half of the mass of biomass consumed.[23] Concentrations of all other emissions in smoke are then relativized to the concentration of the major carbon emission components after being background-corrected. When colocated sampling of microbe concentrations is conducted concurrently with measurement of carbon emissions in smoke, the carbon mass balance approach can also be applied to microbial aerosols to estimate their emission factors.

To demonstrate this approach for microbial emission factor development, this research focused on bacterial emission factors (BEFs) using viable and total bacterial cell data collected in smoke sampled over three prescribed burns and one pile burn.[3] We then scaled up these measurements to extrapolate total and viable annual bacterial emissions from wildland fires and compared the emission rates to global estimates of bacterial emissions from other sources. While only viable microbes have the potential to colonize deposition environments, the transport of non-viable microbes is also relevant due to the persistence of allergenic properties for their aerosols, as well as the atmospheric implications of their activity as ice nucleation particles.[3,4,24,25] Finally, we demonstrate the utility of applying BEFs for the prediction of dispersal and deposition using a newly developed adaptive Langevin dynamics[26] model that is coupled with the fire behavior-atmosphere model WRF-SFIRE.[27] BEFs and their drivers, such as bacterial source concentrations and viability, fire behavior, and atmospheric conditions, will need to be investigated in different regions and fuel types to fully characterize wildland-fire-emitted microbes and the extent of any downwind repercussions.

MATERIALS AND METHODS

Site Description. In June 2019, high-intensity prescribed burns were conducted in the Fishlake National Forest, UT, to reduce hazardous fuel accumulations and restore patches of quaking aspen (*Populus tremuloides*). The burned areas were dominated by subalpine fir (*Abies lasiocarpa*), Engelmann spruce (*Picea engelmannii*), and quaking aspen, with a sparse understory of grasses, shrubs, and saplings. The combined effects of a western spruce budworm outbreak and 50 years of fire suppression led to a high accumulation of large downed woody fuels, which contributed to the high intensity of the burns (Figure S1). Two burns were ignited using terra-torches on ATVs in two isolated hills ("South Knob" and "North Knob", 3 and 23 ha, respectively), while helicopter ignitions were used to ignite a 982 ha Manning Creek unit (Figure S1). Two large slash piles from the previous season's forest thinning treatments were also sampled ("Pile"). Active crown fire behavior characterized by flaming combustion with flame heights extending above the forest canopy was observed in all burn units during sample acquisition. Additional details can be found in Aurell et al.[28] and Kobziar et al.[3] Environmental conditions are summarized in Table S1.

Fuel Loading and Composition. In order to determine patterns of emissions, the consumption of biomass must be assessed.[29] Trees, ground ("duff" or Oe and Oa horizons of soil and anything buried within), and surface fuel (litter, downed woody debris, low-stature vegetation) masses were determined at 61 plot locations that were systematically placed within the three operational burn units between 2017 and 2019. Postfire fuel measurements were also collected in 2019−2021, 20 of which were located inside the Manning Creek unit. Fuel consumption was calculated for each fuel category using modified standard methods[30] described in the Supporting Information.

Light Detection and Ranging-Based Fuel Consumption. The field sample plots represented the range of fuel conditions within the three burn units studied here, but only 20 plots were located in an area sampled for microbe emissions. Therefore, the pre- and postfire field data were pooled into a single data set that more fully represented the range of unburned and burned forest fuel conditions.[31] These plot-level fuel estimates were then used to train an empirical model predicting fuel loading from both pre- and postfire airborne Light Detection and Ranging (LIDAR) data which enabled the estimation of consumption across the full extent of the burn units at 10 m resolution.[31] Fuel loading measurements were used to scale spatially explicit bacterial emissions to each burn unit. Fuel load and consumption data were not available for the Pile burn. Additional details can be found in the Supporting Information.

Smoke Sampling and Quantification of Bacterial Cells. Pilots positioned a DJI Matrice 600 Pro Unmanned Aircraft System (UAS) above tree canopies in the smoke plume based on real-time measurements of elevated CO_2 relayed to the ground using the smoke sampling system described in Nelson et al.[32] A detailed description of the airborne microbe sampling payload and approach can be found in Kobziar et al.[3] To assess background (ambient) concentrations of all aerosols and gases, ambient air was sampled using the same system the day before and the morning of the Pile burn prior to ignition (6/17−6/18).[32] Air was sampled using the Leland Legacy compensating vacuum pump (SKC Inc., Eighty-Four, PA) onto 1.0 μm pore size polycarbonate filters through "button" personal aerosol sampling devices equipped with a steel mesh cover dome with holes sized ∼320 μm (SKC Inc., Eighty-Four, PA). The pump was calibrated to a flow rate of 8 L min^{-1} at the location where sampling took place using a Sensidyne Go-Cal Air Flow Calibrator (Sensidyne LP, St. Petersburg, FL), and the flow rate was split between two button samplers at the recommended 4 L min^{-1} for the samplers as per the manufacturer's specifications to follow the ISO 7708/CEN inhalability curve.[33] Activation of the pump was delayed until the UAS was in the smoke plume and ended before the UAS exited the plume. Height above ground level ranged from 20 to 60 m during the Pile burns (n = 3 flights), 45 to 160 m during the Knob burns (n = 9), and 30 to 100 m during the Manning Creek burns (n = 3). The duration of sampling lasted 5 min due to flight time restrictions, to maximize replicates, and in an attempt to maintain viability of cells deposited on filters.[3] The characteristics of all bioaerosol sampling devices may impact results; however, the button sampler was chosen for its high collection efficiency for bacterial cells and its low sensitivity to surrounding winds such as those created by UAS rotors.[34,35]

https://doi.org/10.1021/acs.est.3c05142
Environ. Sci. Technol. 2024, 58, 2413−2422

Concurrent sampling using the same model DJI Matrice 600 Pro UAS was conducted in the same smoke plumes using the "Kolibri" system described in detail in Aurell et al.[36] and in Supporting Information: Methods. The Kolibri system measurements used for this study included total carbon (elemental plus organic carbon), CO_2, and CO concentrations, from which total carbon mass in smoke as well as background ambient air was quantified for a given air volume using the carbon mass balance method.[36] The UAS carrying the Kolibri system was positioned within <50 m of the UAS used to collect bacterial samples. We selected data from Kolibri measurements that were most contemporaneous with the bacterial payload sampling period in the same smoke plume over the same fuels while fire behavior was similar. Flaming combustion was the predominant phase during all measurements. All measurements from the Kolibri reflect time-integrated values over 5−15 min to characterize mean values in environmental, smoke, and fire conditions.

Once transported to the lab on dry ice (ca. −80 °C), smoke and ambient air filters were vortexed in phosphate-buffered saline solution to disassociate cells from filters as described in Moore et al.[4] The solutions were then filtered in triplicate and stained to enumerate bacterial cells and to identify both total and viable cells based on membrane integrity as described in Kobziar et al.[3] Cell counts were background-corrected based on cell counts derived from ambient air samples to isolate smoke-emitted cells from those regularly occurring in the air.[37] The mean number of cells in these ambient samples was 1.62×10^4 and 1.24×10^4 m^{-3} for total and viable cells, respectively. Any cells found on procedural and field blanks were also subtracted.

Bacterial Emission Factors. A modified version of the carbon mass balance method[36,38] was used to calculate bacterial emission factors (BEFs). Background-corrected cell measurements are equivalent to excess mixing ratios commonly used in smoke emission factor determinations.[39]

$$\mathrm{BEF}_{\mathrm{cells}} = f_c \times \frac{\mathrm{cells}_{n,g}}{g_C} = \frac{\mathrm{cells}_{n,g}}{g_{\mathrm{biomass\ consumed}}} \quad (1)$$

where $\mathrm{BEF}_{\mathrm{cells}}$ in mass (g) or count (n) of cells g^{-1} fuel consumed is determined by f_c = mass fraction of carbon in the fuels consumed, $\mathrm{cells}_{n,g}$ = background-corrected cell concentration by count (n) or mass (g) m^{-3}, and g_C = background-corrected carbon concentration (mass C m^{-3}) based on CO, CO_2, and total carbon content sampled from Aurell et al.[36]

Bacterial cell mass was taken from the literature to be approximately 6.0×10^{-14} g assuming carbon content is approximately 50% of total cell mass.[40] The number of cells was multiplied by the mass per cell to arrive at the cell mass in g m^{-3}. To determine landscape patterns of bacterial emissions, we followed conventional methods of multiplying the BEFs by fuel consumption values per unit area.[39] The detailed fuel consumption data provided by LIDAR and field sampling enabled estimates of bacterial emissions for each pixel in each burn unit to demonstrate the heterogeneity of fuel consumption across the landscape.

Smoke Sample Fetch and Emission Rates. To estimate the mass of fuel consumed that 1 m^3 of smoke represents, we doubled the total carbon mass measured by the EPA Kolibri system to estimate the mass of biomass consumed on the ground per volume of smoke sampled.[36] This mass could then be used in conjunction with the LIDAR-based average fuel consumption values in g m^{-2} for each burn to derive the equivalent ground area of fuel burned per unit volume of smoke sampled. To estimate the bacterial emission rate, Einstein's equation for molecular diffusion derived from Fick's law was employed using a turbulent diffusion coefficient (K_z) as described in Jacob.[41] Sesartic and Dallafior[42] also used this method to estimate spore flux in nonfire conditions. The equation is described in the Supporting Information.

Statistics. Data were analyzed using the NCSS 2021 Statistical analysis package (NCSS, LLC.; ncss.com/software/ncss) and in the R environment. Data were tested for normality and for equal variance among groups (fire type) and were compared using ANOVA. If tests for normality and equal variances were not passed, differences among groups were tested using the Kruskal−Wallis One-Way ANOVA ("K−W") on ranks. If normally distributed with unequal variances, Welch's test of means was employed to test for differences among data categories. Significance was determined at the $p < 0.05$ level.

Modeling Bacterial Transport. A highly scalable and adaptive Lagrangian numerical framework was developed to represent the transport and deposition of the aerosolized bacteria emitted through the interactions between combusting wildland fuels and the boundary layer. Model details are provided in the Supporting Information. In brief, WRF-SFIRE,[27] a coupled fire-atmosphere fire behavior model, was used to simulate fire progression, velocity fields, and heat flux as inputs for the particle transport model. The simulation used in this study was one of the operational forecasts conducted using the WRFx[43] forecasting system in support of the Fire and Smoke Model Evaluation Experiment (FASMEE).[44] For each timestamp of the simulated fire progression, the particles were initialized uniformly throughout the active fire areas, where the modeled heat flux (GRNHFX variable in WRF-SFIRE) was greater than zero. Five million particles were initialized per timestamp of WRF-SFIRE to represent the spatial ensemble of the trajectories in the domain. One hundred timestamps were run resulting in a total simulation of 500 M particles released. The number of particles was selected arbitrarily, and further work is needed to establish the statistical significance of the number of released particles.

To normalize modeling projections from particles to bacterial cells, we used the fuel consumption values from WRF-SFIRE for the Manning Creek fire and multiplied this by the mean bacterial emission factors derived for Manning Creek to estimate total bacterial emissions for the modeled fire area. These values were then used to create a ratio between the total number of particles emitted during the model simulation and the number of bacterial cells emitted from the fuel consumed per unit area. The ratio was used to normalize the arbitrary number of released particles to measured bacterial cells.

RESULTS AND DISCUSSION

Results. *Fuel Loading and Consumption.* Consumption at the 20 repeat measurement plots in the Manning Creek unit ranged from 0 to 123.0 Mg ha^{-1} for downed woody debris, from 1.1 to 4.5 Mg ha^{-1} for litter, from 6.4 to 81.6 Mg ha^{-1} for duff, and from 17.5 to 69.4 Mg ha^{-1} for trees and saplings. The largest contributions to total fuel consumed were duff, trees, and saplings, as well as 1000 h fuels which together comprised 86.5% of the total fuel consumed (Figure S2 and Table S2). LIDAR-based fuel consumption was predicted at each prescribed burn unit. Total mean fuel consumption in burned

https://doi.org/10.1021/acs.est.3c05142
Environ. Sci. Technol. 2024, 58, 2413−2422

areas was 89.93, 89.30, and 108.2 Mg ha^{-1} for the South Knob, North Knob, and Manning Creek units, respectively. Maximum consumption was 218.2 Mg ha^{-1} at the North Knob, 218.4 Mg ha^{-1} at the South Knob, and 336.8 Mg ha^{-1} at the Manning Creek unit. LIDAR-based fuel consumption values were used for all subsequent calculations to maintain consistent methodology among the three burn units (since measurement plots were not installed in the Knob burns).

Bacterial Emission Factors. Total (viable plus dead cells) BEFs (μg cells kg^{-1} fuel) differed significantly among some burn types (K−W test, $p = 0.02$), as did viable BEFs ($F(2, 7) = 29.1$, $p \leq 0.0004$) (Figure 1). Viable cell emission factors were

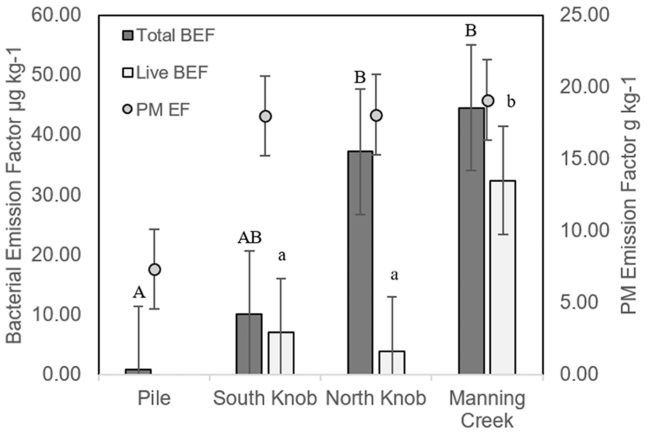

Figure 1. Bacterial emission factors (μg kg^{-1} ± SE) for background-corrected total cells and viable ("live") bacterial cells (bars), and $PM_{2.5}$ emission factors (g kg^{-1}) mean values (circles; from Aurell et al.[28]) across four different burns in the Fishlake National Forest, Utah, USA. Letters represent statistical differences ($p < 0.05$) among burn units. The viability of cells was not assessed in Pile burn samples.

higher in the Manning Creek unit than either of the Knob burns and total cells were lower in the Pile burn than the North Knob and Manning Creek (Tukey−Kramer test, $p < 0.05$). Particulate matter concentrations or EFs did not correlate with BEFs for either live or total bacterial emissions across the burn types.

Across burn types, variability in BEFs was high, as shown by standard deviations close to mean values (Table 1). Because BEFs were also the highest in the Manning Creek burn, total bacterial emissions followed the pattern of increasing total fuel consumed (Figure 1 and Table 1). Fire radiative power (FRP), as assessed from the Hazard Mapping System product, derived from satellite data by the National Oceanic and Atmospheric Administration (NOAA), was nearly an order of magnitude higher in the Manning Creek unit (mean 106.4 ± 122.3 MW) than in the Knob burns (mean 11.0 ± 3.3 MW) and previous work showed higher $PM_{2.5}$ emission factors in Manning Creek than the Knob burns.[28]

Wildland fires in the same ecosystem/fuel types in the Fishlake National Forest burn an average of 2631 ha (as prescribed burns or wildfires) annually (USDA Forest Service records; Richfield Ranger District, Richfield, Utah). Using derived BEF values, this equates to an estimated mean (range) of 1.35×10^{17} (9.74×10^{16}−6.16×10^{18}) total bacteria, or 8.10 (5.84−396.60) kg of bacterial biomass each year from this specific US Forest Service jurisdiction and forest type.

Distribution of Bacterial Emissions across Units. Within the perimeters of each prescribed burn, areas of unburned fuels were identified, and fire-driven emissions from combustion in unburned pixels were assumed to be zero (Figure 2). The spatial distribution of fuel consumption differed across the burn units, with a higher percentage of unburned pixels within the Manning Creek unit. This is typical of larger burn units with longer burn durations where topography and weather fluctuations can play a significant role in patterns of fuel consumption. Within a given burn perimeter, fire-driven cell emissions therefore ranged across 12 orders of magnitude, reflecting the heterogeneity of fuel consumption that is often overlooked in high-intensity fires (Figure 2). Applying emission factors to fuel consumption per unit area in each burn, cell emissions were 1.52×10^9, 5.54×10^9, and 8.31×10^9 cells m^{-2} for the South Knob, North Knob, and Manning Creek units, respectively.

Emission Rates and Sample Fetch. Emission rates as a function of the turbulent diffusion coefficient (K_z) and mean total (live and dead) cell concentrations across each burn unit are shown in Table S3. On average, the emission rates using a K_z of 10^1 m^2 s^{-1} were 5.92×10^4, 1.89×10^5, and 1.70×10^5 cells m^{-2} s^{-1} for the South Knob, North Knob, and Manning Creek burns, respectively. Using a K_z of 10^1 m^2 s^{-1} reflects neutral atmospheric conditions, which are unlikely to be characteristic across the burn units given that fire produces convective winds that likely increase the rate of diffusion near the combustion zone. These estimates are therefore likely to be conservative. Using a K_z of 1×10^2 m^2 s^{-1} is possibly a more accurate representation. It decreases the vertical transport time from 20 to 2 s for cells to travel 20 m, which increases the average emission rates by an order of magnitude (Table S3). Smoke sample fetch results are described in the Supporting Information.

Model Simulations of Bacterial Dispersal. Simulations of bacterial particle emission and transport during the Manning Creek burn are shown in Figures 3, S3, and S4. The integrated particle locations are recorded every 60 s of the total simulation time, which is approximately 1 day and 21 h. Figure 3a shows the depth-averaged aggregate of the particle counts during the total simulation time. The aggregate plots

Table 1. Bacterial Emission Factors (BEFs) Applied to the Total Size of the Burn Units and Fuels Consumed at the Fishlake National Forest, Utah

burn type (n)	total BEF (cells Mg^{1-})	SD (cells Mg^{-1})	total fuel consumed (Mg)	total bacterial emissions (cells burn^{-1})	live bacterial emissions (g burn^{-1})	total bacterial emissions (g burn^{-1})
Pile (3)	1.39×10^{10}	2.13×10^9				
South Knob (5)	1.69×10^{11}	9.64×10^{10}	1.56×10^2	2.63×10^{13}	1.10×10^0	1.58×10^0
North Knob (4)	6.20×10^{11}	8.63×10^{11}	1.34×10^3	8.32×10^{14}	2.63×10^0	4.99×10^1
Manning Creek (3)	7.68×10^{11}	2.91×10^{11}	3.88×10^4	2.98×10^{16}	1.26×10^3	1.79×10^3

https://doi.org/10.1021/acs.est.3c05142
Environ. Sci. Technol. 2024, 58, 2413−2422

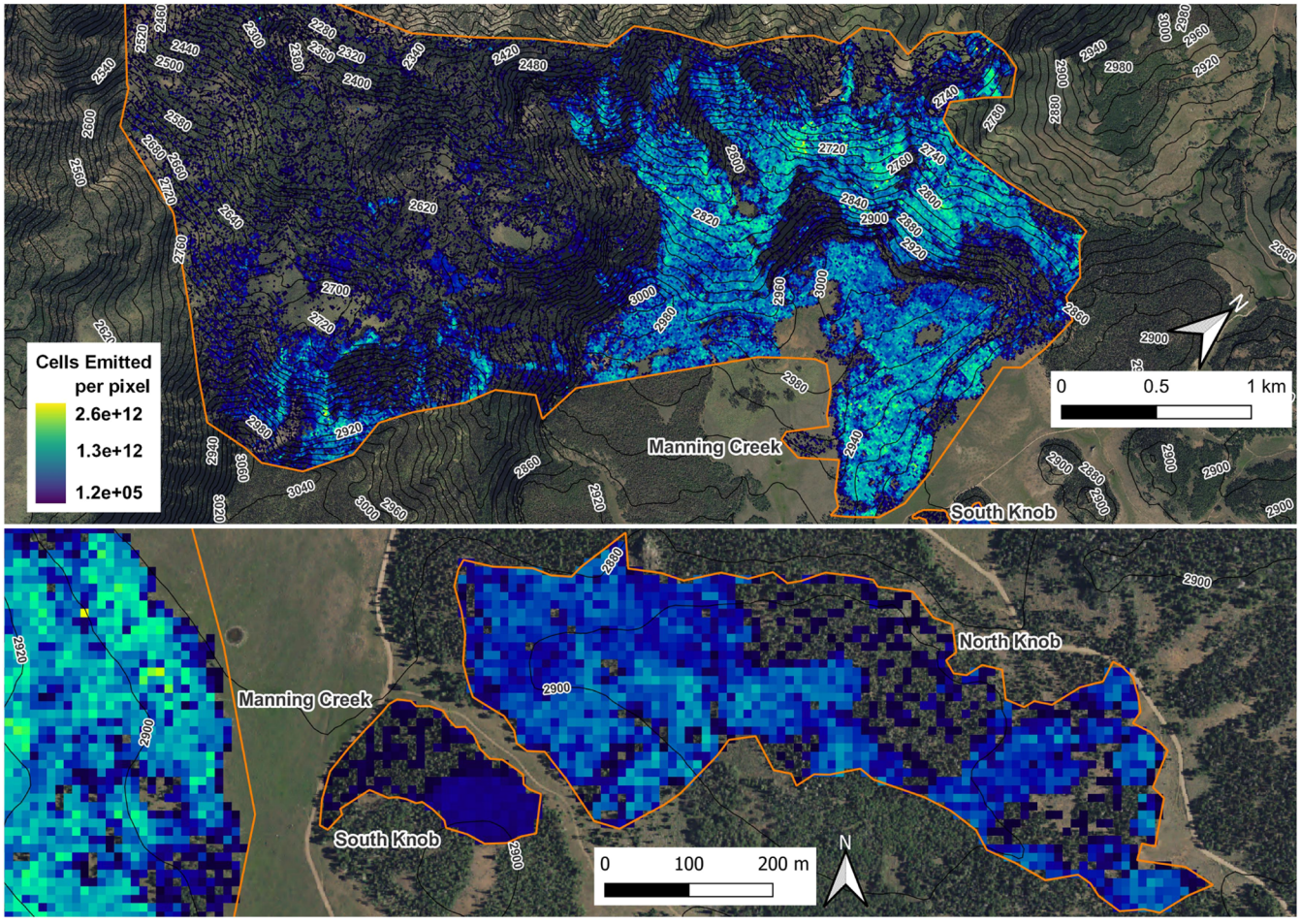

Figure 2. Map of estimated numbers of total bacterial cells emitted per 10 × 10 m^2 pixel based on bacterial emission factors applied to fuel consumption values in Manning Creek (top) and South Knob and North Knob (bottom) burns. Maps assume the relationship between fuel consumption and bacterial emissions is linear. Note: orientation and scale differ between images.

reveal the particles' trajectory signature due to the high spatiotemporal resolution of the outputs, namely, 20 m × 20 m in space and one output per minute.

The simulated Manning Creek burn starts with a high-wind boundary layer from the southwest toward the northeast of the domain, and the wind speed reduces toward the end of the simulation. The combined effect of the high-wind boundary layer and complex terrain leads to the transport of ~2.82 × 10^{17} aerosolized cells outside of the computational domain leaving only 0.0483% to be deposited within the simulation boundary. This behavior is captured in Figure 3, where aggregated trajectory signature is elongated toward the northeast aligned with the dominant wind velocity direction. This result is consistent with the expected behavior from the released particle cloud with Stokes numbers less than unity.

While most of the aggregated count of particles shows deposition close to the fire perimeter (Figure 3b), the spatial distribution of the size of the particles shown in Figure 3c and the standard deviation of the deposited mass and size (Figure S4) indicate that there is no systematic bias in the modeling of deposition patterns. The results demonstrate the dependence of deposition on the complex reciprocating interactions of the fire with the boundary layer and terrain, which is consistent with previous studies.[45,46] In addition, Figure 3c exhibits the full extent of the affected area being significantly larger than that of the burn scar. Notably, Figure 3c shows the landing location patterns of the larger- and smaller-diameter particles. Shortly after the fire ignition, strong winds from southwest to northeast create an advection-driven fire regime initializing all particles with high momentum. As a result, the smaller size and, subsequently, lighter particles leave the computational domain, and the heavier particles that do not leave the domain land farther from the burn perimeter (Figures 3c and Figure S3). The random sampling distribution of the particles' diameter remains the same through the simulation time, and later, when the fire regime is buoyancy-driven, the plume causes larger updrafts and less advective motion toward the boundaries leading to higher lofting elevations and high standard deviation in the mass and diameter of the deposited particles (Figure S4).

Discussion. *Bacterial Emission Factors, Rates, and Fluxes.* This derivation of BEFs establishes a foundation for comparisons with other estimates of bioaerosol emissions, emission fluxes, and relationships between point emissions sources and near-surface aerosolized concentrations. Direct measures of microbial emissions are rare and methods used to determine fluxes are inconsistent and predominantly based on culture-dependent methods rather than direct approaches including microscopy- or flow cytometry.[47,48] Comparisons with other bioaerosol studies are limited by (1) lack of published data on biomass burning microbial emissions or their relationship to fuel consumption and (2) nonfire

https://doi.org/10.1021/acs.est.3c05142
Environ. Sci. Technol. 2024, 58, 2413−2422

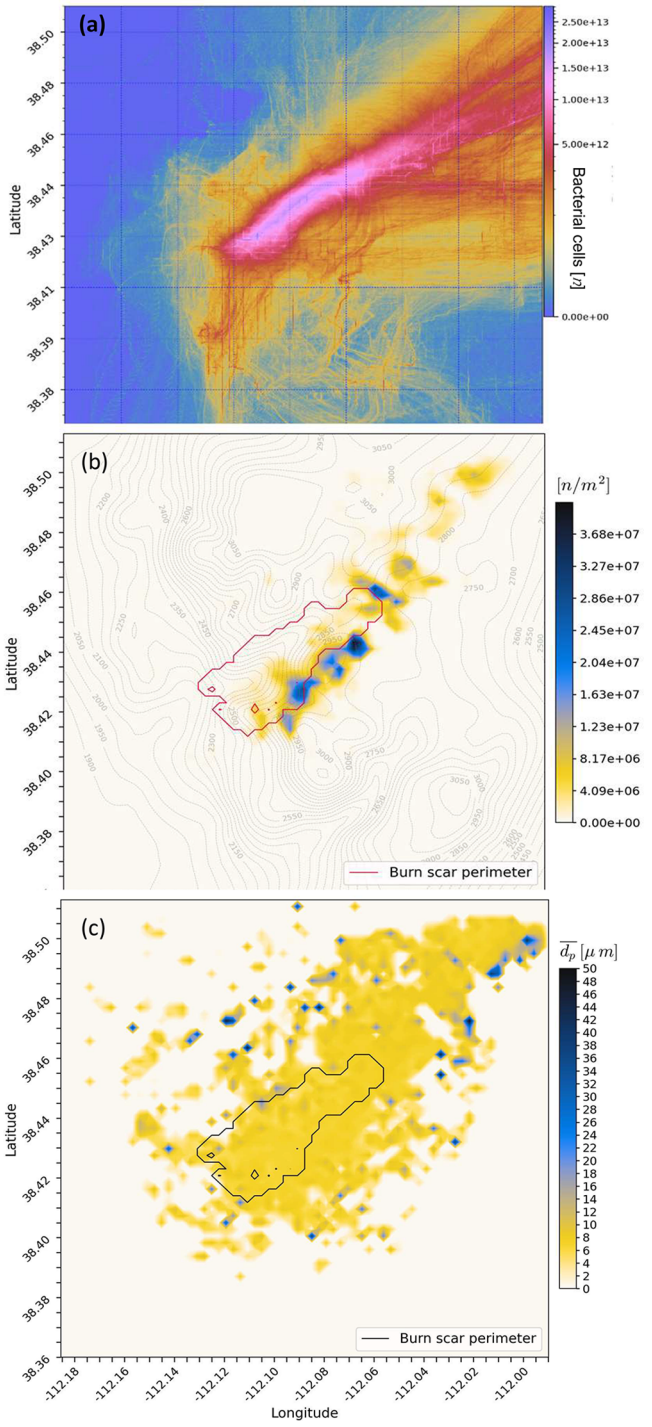

Figure 3. Aggregate spatial distribution of the emitted bacterial particles through the entire simulation time (a). Each pixel in (a) represents a 20 m × 20 m cell within the extent of the computational domain. Modeled number of deposited cells per unit area (b) and the average diameter of deposited cells (c) deposited by the smoke plume of the Manning Creek fire (perimeter is black line polygon) is shown in each 250 × 250 m^2 computational cell in the modeling domain area of 17.25 × 17.25 km^2. Figure S4 shows the standard deviation for deposition particle diameters, and Figures S5 and S6 show plume attachment to terrain for a single example timestamp.

bioaerosol emission rates being estimated per unit area rather than measured from aerosolization mechanisms of a known source. The emissions studied here can be considered point-source emissions since they are corrected for background concentrations. To our knowledge, there exist no similar direct cell quantifications of point sources of bioaerosol emissions normalized to the mass of the source (vegetation, soil, or other source material).

An indirect model-based approach to BEF quantification resulted in estimates within an order of magnitude when compared to that in this study. Moore et al.[4] used a common smoke modeling system, FOFEM,[15] to estimate fuel consumption and associated particulate matter produced for a 1 m^2 area burned in upland pine prescribed burns in Florida, USA. They then extrapolated the concentration of cells based on measured relationships between PM_{10} and cell concentrations in smoke (cells m^{-3}). Estimated cells per unit area burned divided by modeled fuel consumption values in g m^{-2} from Moore et al.[4] would result in an estimated bacterial emission factor of 6.26 × 10^6 cells g^{-1} fuel consumed, compared to this study's derived estimate for subalpine forests averaging 5.19 × 10^5 cells g^{-1}. Differences of this magnitude are not uncommon in emission factors studies and can be related to differences in bacterial loading in the source materials, combustion phase, and fire behavior, as well as different approaches to sampling, analysis, and interpretation of emissions.[11,36,49] The fact that Moore et al.[4] did not account for background cell concentrations, which would have reduced the BEFs ∼5-fold, may help explain the difference in BEFs between the studies, in addition to higher intensity fire presumably destroying some of the cells in this study.

The limited published studies[47,48] where bacterial emission fluxes have been reported were compiled from culturable bacteria or gene copy counts from qPCR, and therefore, are not directly comparable to the cell counts obtained by microscopy in this study. Ambient air emission rates for bacterial cell counts have, however, been simulated using the EMAC model using arbitrary emission rates normalized to empirically derived cell concentrations in air compiled from other studies.[50] Results from those simulations estimate that bacterial emission rates from global ecosystems range from 140 to 380 cells m^{-2} s^{-1} with annual emissions accumulating to 1.4 × 10^{24} cells from all terrestrial and aquatic ecosystems combined.[50] The estimated total bacterial cell emission rates from this study's wildland fires based on measured consumption levels of source materials (with mean fluxes ranging from 5.9 × 10^4 to 1.7 × 10^6 cells m^{-2} s^{-1}, Table S3) exceed these emission rates by 2−4 orders of magnitude. If the BEFs derived in this study are extrapolated to global annual wildland fire area burned,[7] our estimates would equate to between 6.31 × 10^{21} and 3.45 × 10^{22} cells emitted annually during fire events from burned terrestrial sources similar to the forests and fires considered here. The representativeness of these estimates is limited by the lack of any prior published data on bacterial emission rates from other types and conditions of wildland fires, and therefore should be interpreted with caution since actual rates are likely to vary considerably among different fires burning different fuels.

Bacterial emission rates reported here reflect the combined influence of three key processes. First, vegetation and other fuels (e.g., the O horizons of soils) are physically broken down during combustion, exposing microbes previously not susceptible to passive or active aerosolization mechanisms to a turbulent environment. These include endophytic organisms and those within organic soil horizons such as the Oa/Oe layers ("duff"), which comprised nearly a quarter of the total

https://doi.org/10.1021/acs.est.3c05142
Environ. Sci. Technol. 2024, 58, 2413−2422

fuel load consumed in the Manning Creek burn (Table S2). Second, microbes are driven into the smoke plume attached to products of incomplete combustion, such as fire-derived particulate matter, which would not be emitted without fire. Third, strong convective winds in and around the combustion zone can aerosolize microbes from both intact source surfaces (including soils) and those that have been newly exposed. Together, these processes increase both the susceptibility of source microbes to aerosolization mechanisms and the degree of aerosolization during wildland fires well above background levels.

Bacterial cell emission factors differed significantly among fire types (Figure 1) because the fires burned differently, as documented by the variability in their fuel consumption (Figure 2). Spatial variability in fuel consumption can be explained by factors such as heterogeneous fuel distribution and composition, topography, ignition techniques, burn period weather, and time of day. This spatiotemporal variability is also reflected in the estimated bacterial emissions by utilizing BEFs, as shown in Figure 2. The combined results of spatially explicit fuel consumption estimates and the variability in BEFs across the samples (Table 1) reveal the complexity of bacterial emissions during both small and large wildland fires. Further studies are required to determine whether the values derived here are representative of other fuel types and fire conditions.

Modeling Smoke Bacterial Dispersal and Transport. The particle transport modeling domain used in this study covers an area centered on the burn of 17.25 x 17.25 km and predicts that less than 0.05% of the bacteria aerosolized would have been deposited within that zone. The fate of the aerosolized microbes beyond the domain is unknown; however, modeling projects from other authors for non-ice nucleating, non-CCN aerosolized bacteria above forests suggest that the duration of suspension can last from weeks up to 166 days.[50] The degree to which observed microbes and aggregates of microbes remain clumped, coagulate, or separate as a plume ages remains a significant unknown and has important consequences to the prediction of deposition and longer-distance dispersal. The strong influence of the boundary layer winds on aerosolized particles suggests that increasing the size of the computational domain and the total simulation time would be needed to fully characterize the fate of the transported bacteria.

The presented modeling framework integrating a coupled fire-atmosphere model with the new high-fidelity particle transport model creates a novel capability to support hypothesis testing and can accommodate a range of BEFs aligned with predicted or observed fire behavior. For example, it can provide forecasts of the expected dispersion of key microbes of interest (e.g., pathogens) from a prescribed burn or a wildfire. Additionally, the presented high-resolution coupled system could be integrated into large-scale global climate models to inform the effects of brown carbon[25] on atmospheric processes.[4,51] The model coupling demonstrated here serves as a foundation to enable numerical studies focused on the impacts of fire-related microbe emission and dispersion on microphysics, the radiative budget, and global climate.

Comparisons with North American and Global Mass of Bacterial Emissions. Using estimates for annual wildland fire biomass consumption from van Wees et al.[7] and the overall range of BEFs derived here, we estimate annual bacterial emissions for North America to range between 1.48×10^{-01} Mg and 8.26×10^{0} Mg, or global equivalents of 4.57×10^{1} to 2.55×10^{3} Mg. Andreae and Merlet[52] also estimated the annual vegetative biomass consumed in wildland fires globally across major ecosystem types. The forests studied here fall into the "extratropical forest" category, for which Andreae and Merlet[49] estimate the mass consumed annually at 6.4×10^{8} Mg resulting in estimated annual bacterial emissions from similar forests ranging between 1.31×10^{0} and 7.30×10^{1} Mg.

To compare the values derived here with non-fire estimates for annual background aerosolization of bacterial mass, considerations must include the proportion of the earth's surface represented and the fact that existing nonfire estimates represent the sum of constant bioaerosol emissions rather than episodic emission events such as wildland fire. Using values from van Wees et al.[7] for the portion of Earth's total area burned annually (7.84×10^{-3}), we can normalize estimates from other studies to an equivalent area of daily emissions to compare fire and nonfire mechanisms directly. For example, if the Burrows et al.[50] estimated global 1.10×10^{-1} to 4.931 −-4.93 Gg day^{-1} of emitted bacteria are normalized to the area burned in wildland fire,[7] mean bacterial emissions from fire based on the BEFs dervied here would exceed daily background emissions by 5.90×10^{2} to 6.28×10^{2} Mg . Although these results do not factor in the likely high degree of variability of BEFs across different ecosystems and burning conditions, the estimates suggest that the contribution of wildland fire to bacterial emissions from terrestrial sources is likely significant. The fire mechanism for bacterial emission has likely been acting for over 400 M years or as long as fires have consumed organic biomass across landscapes.

LIMITATIONS AND OPPORTUNITIES

These BEFs are representative of the atmospheric conditions, fuels and bacterial source content, and fire behavior particular to the fires in this study, and do not include the potentially significant contributions to overall mass/concentrations of other biological emissions found in smoke[5,51] (e.g., fungi, pollen, archaea, microfauna, viruses). Emission factors in general vary depending on fire behavior, combustion phases, and the composition of fuels and their environments.[11] Although the fires in this study ranged higher in fire intensity than many prescribed burns,[51] the size and weather conditions characterizing these burns do not compare to large wildfires (e.g., > 10,000 ha) burning under extreme weather conditions. Smoke from extreme wildfires can travel beyond the tropopause and distribute suspended emissions across continents.[53] Sampling directly from sources and at multiple distances from combustion zones on large wildfires would yield informative results for comparison with the fire conditions represented in this study and for modeling their longer-distance transport.

ASSOCIATED CONTENT

Supporting Information

The Supporting Information is available free of charge at https://pubs.acs.org/doi/10.1021/acs.est.3c05142.

Photos of fire behavior, smoke, and postfire conditions; details of methods including model development; supporting results including sampling fetch analysis; and discussion (PDF)

https://doi.org/10.1021/acs.est.3c05142
Environ. Sci. Technol. 2024, 58, 2413−2422

AUTHOR INFORMATION

Corresponding Author

Leda N. Kobziar − *Department of Natural Resources and Society, University of Idaho, Coeur d'Alene, Idaho 83814, United States;* orcid.org/0000-0002-5882-8498; Email: lkobziar@uidaho.edu

Authors

Phinehas Lampman − *Department of Natural Resources and Society, University of Idaho, Coeur d'Alene, Idaho 83814, United States*

Ali Tohidi − *Mechanical Engineering Department, Wildfire Interdisciplinary Research Center, San Jose State University, San Jose, California 95192, United States*

Adam K. Kochanski − *Department of Meteorology and Climate Science, Wildfire Interdisciplinary Research Center, San Jose State University, San Jose, California 95192, United States*

Antonio Cervantes − *Mechanical Engineering Department, Wildfire Interdisciplinary Research Center, San Jose State University, San Jose, California 95192, United States*

Andrew T. Hudak − *Rocky Mountain Research Station, USDA Forest Service, Moscow, Idaho 83846, United States*

Ryan McCarley − *Department of Forest, Fire and Rangeland Sciences, University of Idaho, Moscow, Idaho 83844, United States*

Brian Gullett − *Office of Research and Development, Environmental Protection Agency, Research Triangle Park, North Carolina 27711, United States;* orcid.org/0000-0003-4547-4026

Johanna Aurell − *Office of Research and Development, Environmental Protection Agency, Research Triangle Park, North Carolina 27711, United States*

Rachel Moore − *Department of Microbiology and Cell Science, University of Florida, Gainesville, Florida 32611, United States*

David C. Vuono − *Department of Civil and Environmental Engineering, Colorado School of Mines, Golden, Colorado 80401, United States*

Brent C. Christner − *Department of Microbiology and Cell Science, University of Florida, Gainesville, Florida 32611, United States;* orcid.org/0000-0002-9894-7360

Adam C. Watts − *Pacific Northwest Research Station, USDA Forest Service, Wenatchee, Washington 98801, United States*

James Cronan − *Pacific Northwest Research Station, USDA Forest Service, Seattle, Washington 98103, United States*

Roger Ottmar − *Pacific Northwest Research Station, USDA Forest Service, Seattle, Washington 98103, United States*

Complete contact information is available at: https://pubs.acs.org/10.1021/acs.est.3c05142

Notes

The authors declare no competing financial interest.

ACKNOWLEDGMENTS

The authors thank Jesse Juchtzer, Dave Page, and Patrick Melarkey from the Desert Research Institute for piloting the UAS. Fishlake National Forest personnel including managers, fire crews, and IMT members are recognized for their critical roles. EPA Office of Research and Development and USDA Forest Service Joint Venture Agreement 20-JV-11261987-115 provided funding. The authors acknowledge high-performance computing support from Cheyenne (doi: 10.5065/D6RX99HX) and the SJSU Fire HPC Support group for providing computational assistance. This work was funded in part by NSF Grants DEB-2039552, DEB-2039525, and IUCRC-2113931, as well as NASA Grants 80NSSC19K1091 and 80NSSC22K1717. Thanks go to Jennifer Andrew.

REFERENCES

(1) Griffin, D. W. Atmospheric Movement of Microorganisms in Clouds of Desert Dust and Implications for Human Health. *Clin. Microbiol. Rev.* **2007**, *20* (3), 459−477.

(2) Brown, G. S.; Mohr, A. J. Fate and Transport of Microorganisms in Air. In *Manual of Environmental Microbiology*; John Wiley & Sons, Ltd., 2016 ; pp 3.2.4-1−3.2.4-12.

(3) Kobziar, L. N.; Vuono, D.; Moore, R.; Christner, B. C.; Dean, T.; Betancourt, D.; Watts, A. C.; Aurell, J.; Gullett, B. Wildland Fire Smoke Alters the Composition, Diversity, and Potential Atmospheric Function of Microbial Life in the Aerobiome. *ISME Commun.* **2022**, *2* (1), 8.

(4) Moore, R. A.; Bomar, C.; Kobziar, L. N.; Christner, B. C. Wildland Fire as an Atmospheric Source of Viable Microbial Aerosols and Biological Ice Nucleating Particles. *ISME J.* **2021**, *15*, 461.

(5) Kobziar, L. N.; Pingree, M. R. A.; Larson, H.; Dreaden, T. J.; Green, S.; Smith, J. A. Pyroaerobiology: The Aerosolization and Transport of Viable Microbial Life by Wildland Fire. *Ecosphere* **2018**, *9* (11), No. e02507.

(6) Camacho, I.; Góis, A.; Camacho, R.; Nóbrega, V.; Fernandez, G. The Impact of Urban and Forest Fires on the Airborne Fungal Spore Aerobiology. *Aerobiologia* **2018**, *34* (4), 585−592, DOI: 10.1007/s10453-018-9530-x.

(7) van Wees, D.; van der Werf, G. R.; Randerson, J. T.; Rogers, B. M.; Chen, Y.; Veraverbeke, S.; Giglio, L.; Morton, D. C. Global Biomass Burning Fuel Consumption and Emissions at 500 m Spatial Resolution Based on the Global Fire Emissions Database (GFED). *Geosci. Model Dev.* **2022**, *15* (22), 8411−8437.

(8) van der Werf, G. R.; Randerson, J. T.; Giglio, L.; van Leeuwen, T. T.; Chen, Y.; Rogers, B. M.; Mu, M.; van Marle, M. J. E.; Morton, D. C.; Collatz, G. J.; Yokelson, R. J.; Kasibhatla, P. S. Global Fire Emissions Estimates during 1997−2016. *Earth Syst. Sci. Data* **2017**, *9* (2), 697−720.

(9) Akagi, S. K.; Yokelson, R. J.; Wiedinmyer, C.; Alvarado, M. J.; Reid, J. S.; Karl, T.; Crounse, J. D.; Wennberg, P. O. Emission Factors for Open and Domestic Biomass Burning for Use in Atmospheric Models. *Atmos. Chem. Phys.* **2011**, *11* (9), 4039−4072.

(10) Yokelson, R. J.; Burling, I. R.; Gilman, J. B.; Warneke, C.; Stockwell, C. E.; de Gouw, J.; Akagi, S. K.; Urbanski, S. P.; Veres, P.; Roberts, J. M.; Kuster, W. C.; Reardon, J.; Griffith, D. W. T.; Johnson, T. J.; Hosseini, S.; Miller, J. W.; Cocker III, D. R.; Jung, H.; Weise, D. R. Coupling Field and Laboratory Measurements to Estimate the Emission Factors of Identified and Unidentified Trace Gases for Prescribed Fires. *Atmos. Chem. Phys.* **2013**, *13* (1), 89−116.

(11) Prichard, S. J.; O'Neill, S.; Eagle, P.; Andreu, A.; Drye, B.; Dubowey, J.; Urbanski, S.; Strand, T. Wildland Fire Emission Factors in North America: Synthesis of Existing Data, Measurement Needs and Management Applications. *Int. J. Wildland Fire* **2020**, *29* (2), 132−147.

(12) Stein, A. F.; Draxler, R. R.; Rolph, G. D.; Stunder, B. J. B.; Cohen, M. D.; Ngan, F. NOAA's HYSPLIT Atmospheric Transport and Dispersion Modeling System. *Bull. Am. Meteorol. Soc.* **2015**, *96* (12), 2059−2077.

(13) Prichard, S. J.; Karau, E. C.; Ottmar, R. D.; Kennedy, M. C.; Cronan, J. B.; Wright, C. S.; Keane, R. E. Evaluation of the CONSUME and FOFEM Fuel Consumption Models in Pine and Mixed Hardwood Forests of the Eastern United States. *Can. J. For. Res.* **2014**, *44* (7), 784−795.

(14) Larkin, N. K.; O'Neill, S. M.; Solomon, R.; Raffuse, S.; Strand, T.; Sullivan, D. C.; Krull, C.; Rorig, M.; Peterson, J.; Ferguson, S. A.

The BlueSky Smoke Modeling Framework. *Int. J. Wildland Fire* **2009**, *18* (8), 906−920, DOI: 10.1071/WF07086.
(15) Reinhardt, E. D.; Keane, R. E.; Brown, J. K. *First Order Fire Effects Model: FOFEM 4.0, User's Guide, INT-GTR-344* U.S. Department of Agriculture, Forest Service, Intermountain Research Station: Ogden, UT; 1997.
(16) Kobziar, L. N.; Thompson, G. R. Wildfire Smoke, a Potential Infectious Agent. *Science* **2020**, *370* (6523), 1408−1410.
(17) Hauser, N.; Conlon, K. C.; Desai, A.; Kobziar, L. N. <p > Climate Change and Infections on the Move in North America. *Infect. Drug Resist.* **2021**, *14*, 5711−5723.
(18) Aylor, D. E.; Schmale, D. G.; Shields, E. J.; Newcomb, M.; Nappo, C. J. Tracking the Potato Late Blight Pathogen in the Atmosphere Using Unmanned Aerial Vehicles and Lagrangian Modeling. *Agric. For. Meteorol.* **2011**, *151* (2), 251−260.
(19) Pearce, D. A.; Alekhina, I. A.; Terauds, A.; Wilmotte, A.; Quesada, A.; Edwards, A.; Dommergue, A.; Sattler, B.; Adams, B. J.; Magalhães, C.; Chu, W.-L.; Lau, M. C. Y.; Cary, C.; Smith, D. J.; Wall, D. H.; Eguren, G.; Matcher, G.; Bradley, J. A.; de Vera, J.-P.; Elster, J.; Hughes, K. A.; Cuthbertson, L.; Benning, L. G.; Gunde-Cimerman, N.; Convey, P.; Hong, S. G.; Pointing, S. B.; Pellizari, V. H.; Vincent, W. F. Aerobiology Over Antarctica − A New Initiative for Atmospheric Ecology. *Front. Microbiol.* **2016**, *7*, No. 16, DOI: 10.3389/fmicb.2016.00016.
(20) Smith, D. J.; Griffin, D. W.; McPeters, R. D.; Ward, P. D.; Schuerger, A. C. Microbial Survival in the Stratosphere and Implications for Global Dispersal. *Aerobiologia* **2011**, *27* (4), 319−332.
(21) Bauer, H.; Giebl, H.; Hitzenberger, R.; Kasper-Giebl, A.; Reischl, G.; Zibuschka, F.; Puxbaum, H. Airborne Bacteria as Cloud Condensation Nuclei. *J. Geophys. Res.* **2003**, *108* (D21), 4658.
(22) Nelson, M., Jr. *An Evaluation of the Carbon Balance Technique for Estimating Emission Factors and Fuel Consumption in Forest Fires* U.S. Department of Agriculture, Forest Service, Southeastern Forest Experiment Station: Asheville, NC; 1982.
(23) Williams, C. L.; Emerson, R. M.; Tumuluru, J. S.; Williams, C. L.; Emerson, R. M.; Tumuluru, J. S. *Biomass Compositional Analysis for Conversion to Renewable Fuels and Chemicals*; IntechOpen, 2017.
(24) Prenni, A. J.; DeMott, P. J.; Sullivan, A. P.; Sullivan, R. C.; Kreidenweis, S. M.; Rogers, D. C. Biomass Burning as a Potential Source for Atmospheric Ice Nuclei: Western Wildfires and Prescribed Burns. *Geophys. Res. Lett.* **2012**, *39* (11), No. L11805, DOI: 10.1029/2012GL051915.
(25) Zhang, Y.; Forrister, H.; Liu, J.; Dibb, J.; Anderson, B.; Schwarz, J. P.; Perring, A. E.; Jimenez, J. L.; Campuzano-Jost, P.; Wang, Y.; Nenes, A.; Weber, R. J. Top-of-Atmosphere Radiative Forcing Affected by Brown Carbon in the Upper Troposphere. *Nat. Geosci.* **2017**, *10* (7), 486−489.
(26) Inci, G.; Kronenburg, A.; Weeber, R.; Pflüger, D. Langevin Dynamics Simulation of Transport and Aggregation of Soot Nano-Particles in Turbulent Flows. *Flow Turbulence Combust.* **2017**, *98* (4), 1065−1085.
(27) Mandel, J.; Amram, S.; Beezley, J. D.; Kelman, G.; Kochanski, A. K.; Kondratenko, V. Y.; Lynn, B. H.; Regev, B.; Vejmelka, M. Recent Advances and Applications of WRF−SFIRE. *Nat. Hazards Earth Syst. Sci.* **2014**, *14* (10), 2829−2845.
(28) Aurell, J.; Gullett, B.; Holder, A.; Kiros, F.; Mitchell, W.; Watts, A.; Ottmar, R. Wildland Fire Emission Sampling at Fishlake National Forest, Utah Using an Unmanned Aircraft System. *Atmos. Environ.* **2021**, *247*, No. 118193.
(29) Surawski, N. C.; Sullivan, A. L.; Roxburgh, S. H.; Meyer, C. P. M.; Polglase, P. J. Incorrect Interpretation of Carbon Mass Balance Biases Global Vegetation Fire Emission Estimates. *Nat. Commun.* **2016**, *7* (1), No. 11536.
(30) Brown, J. K. *Handbook for Inventorying Downed Woody Material*; U.S. Department of Agriculture, Forest Service, Intermountain Forest and Range Experiment Station: Ogden, UT, 1974; Vol. *24*, p 016.
(31) McCarley, T. R.; Hudak, A. T.; Sparks, A. M.; Vaillant, N. M.; Meddens, A. J. H.; Trader, L.; Mauro, F.; Kreitler, J.; Boschetti, L. Estimating Wildfire Fuel Consumption with Multitemporal Airborne Laser Scanning Data and Demonstrating Linkage with MODIS-Derived Fire Radiative Energy. *Remote Sens. Environ.* **2020**, *251*, No. 112114.
(32) Nelson, K.; Boehmler, J.; Khlystov, A.; Moosmüller, H.; Samburova, V.; Bhattarai, C.; Wilcox, E.; Watts, A. A Multipollutant Smoke Emissions Sensing and Sampling Instrument Package for Unmanned Aircraft Systems: Development and Testing. *Fire* **2019**, *2* (2), 32.
(33) International Organization for Standardization. Air Quality − Particle Size Fraction Definitions for Health-Related Sampling (ISO Standard No. 7708:1995) 1995 https://www.iso.org/standard/14534.html.
(34) Aizenberg, V.; Reponen, T.; Grinshpun, S. A.; Willeke, K. Performance of Air-O-Cell, Burkard, and Button Samplers for Total Enumeration of Airborne Spores. *AIHA J.* **2000**, *61* (6), 855−864.
(35) Aizenberg, V.; Choe, K.; Grinshpun, S. A.; Willeke, K.; Baron, P. A. Evaluation of Personal Aerosol Samplers Challenged with Large Particles. *J. Aerosol Sci.* **2001**, *32* (6), 779−793.
(36) Aurell, J.; Gullett, B.; Holder, A.; et al. Wildland Fire Emission Sampling at Fishlake National Forest, Utah Using an Unmanned Aircraft System. *Atmos. Environ.* **2021**, *247*, No. 118193, DOI: 10.1016/j.atmosenv.2021.118193.
(37) Jones, A. M.; Harrison, R. M. The Effects of Meteorological Factors on Atmospheric Bioaerosol Concentrations—a Review. *Sci. Total Environ.* **2004**, *326* (1), 151−180.
(38) Ward, D. E. In *Projections of Emissions from Burning of Biomass for Use in Studies of Global Climate and Atmospheric Chemistry*, Annual Meeting of the Air and Waste Management Association Canada, Vancouver, British Columbia, 1991; p 19.
(39) *Wildland Fire Smoke in the United States: A Scientific Assessment*; Peterson, D. L.; McCaffrey, S. M.; Patel-Weynand, T., Eds.; Springer International Publishing: Cham, 2022.
(40) Bar-On, Y. M.; Phillips, R.; Milo, R. The Biomass Distribution on Earth. *Proc. Natl. Acad. Sci. U.S.A.* **2018**, *115* (25), 6506−6511.
(41) Jacob, D. J. *Introduction to Atmospheric Chemistry*; Princeton University Press, 2000.
(42) Sesartic, A.; Dallafior, T. N. Global Fungal Spore Emissions, Review and Synthesis of Literature Data. *Biogeosciences* **2011**, *8* (5), 1181−1192.
(43) Mandel, J.; Vejmelka, M.; Kochanski, A.; Farguell, A.; Haley, J.; Mallia, D.; Hilburn, K.In *An Interactive Data-Driven HPC System for Forecasting Weather, Wildland Fire, and Smoke*, IEEE/ACM HPC for Urgent Decision Making (UrgentHPC), 2019; pp 35−44.
(44) Prichard, S.; Larkin, N. S.; Ottmar, R.; French, N. H. F.; Baker, K.; Brown, T.; Clements, C.; Dickinson, M.; Hudak, A.; Kochanski, A.; Linn, R.; Liu, Y.; Potter, B.; Mell, W.; Tanzer, D.; Urbanski, S.; Watts, A. The Fire and Smoke Model Evaluation Experiment—A Plan for Integrated, Large Fire−Atmosphere Field Campaigns. *Atmosphere* **2019**, *10* (2), 66.
(45) Mell, W.; Jenkins, M. A.; Gould, J.; Cheney, P. A Physics-Based Approach to Modelling Grassland Fires. *Int. J. Wildland Fire* **2007**, *16* (1), 1.
(46) Liu, Y.; Kochanski, A.; Baker, K. R.; Mell, W.; Linn, R.; Paugam, R.; Mandel, J.; Fournier, A.; Jenkins, M. A.; Goodrick, S.; Achtemeier, G.; Zhao, F.; Ottmar, R.; French, N. H. F.; Larkin, N.; Brown, T.; Hudak, A.; Dickinson, M.; Potter, B.; Clements, C.; Urbanski, S.; Prichard, S.; Watts, A.; McNamara, D. Fire Behaviour and Smoke Modelling: Model Improvement and Measurement Needs for next-Generation Smoke Research and Forecasting Systems. *Int. J. Wildland Fire* **2019**, *28* (8), 570−588, DOI: 10.1071/WF18204.
(47) Carotenuto, F.; Georgiadis, T.; Gioli, B.; Leyronas, C.; Morris, C. E.; Nardino, M.; Wohlfahrt, G.; Miglietta, F. Measurements and Modeling of Surface−Atmosphere Exchange of Microorganisms in Mediterranean Grassland. *Atmos. Chem. Phys.* **2017**, *17* (24), 14919−14936.

(48) Burrows, S. M.; Elbert, W.; Lawrence, M. G.; Pöschl, U. Bacteria in the Global Atmosphere − Part 1: Review and Synthesis of Literature Data for Different Ecosystems. *Atmos. Chem. Phys.* **2009**, *9* (23), 9263−9280.
(49) Aurell, J.; Gullett, B. K.; Tabor, D. Emissions from Southeastern U.S. Grasslands and Pine Savannas: Comparison of Aerial and Ground Field Measurements with Laboratory Burns. *Atmos. Environ.* **2015**, *111*, 170−178.
(50) Burrows, S. M.; Butler, T.; Jöckel, P.; Tost, H.; Kerkweg, A.; Pöschl, U.; Lawrence, M. G. Bacteria in the Global Atmosphere − Part 2: Modeling of Emissions and Transport between Different Ecosystems. *Atmos. Chem. Phys.* **2009**, *9* (23), 9281−9297.
(51) Kobziar, L. N.; Vuono, D.; Moore, R.; Christner, B. C.; Dean, T.; Betancourt, D.; Watts, A. C.; Aurell, J.; Gullett, B. Wildland Fire Smoke Alters the Composition, Diversity, and Potential Atmospheric Function of Microbial Life in the Aerobiome. *ISME Commun.* **2022**, *2* (1), 8.
(52) Andreae, M. O.; Merlet, P. Emission of Trace Gases and Aerosols from Biomass Burning. *Global Biogeochem. Cycles* **2001**, *15* (4), 955−966.
(53) Katich, J. M.; Apel, E. C.; Bourgeois, I.; Brock, C. A.; Bui, T. P.; Campuzano-Jost, P.; Commane, R.; Daube, B.; Dollner, M.; Fromm, M.; Froyd, K. D.; Hills, A. J.; Hornbrook, R. S.; Jimenez, J. L.; Kupc, A.; Lamb, K. D.; McKain, K.; Moore, F.; Murphy, D. M.; Nault, B. A.; Peischl, J.; Perring, A. E.; Peterson, D. A.; Ray, E. A.; Rosenlof, K. H.; Ryerson, T.; Schill, G. P.; Schroder, J. C.; Weinzierl, B.; Thompson, C.; Williamson, C. J.; Wofsy, S. C.; Yu, P.; Schwarz, J. P. Pyrocumulonimbus Affect Average Stratospheric Aerosol Composition. *Science* **2023**, *379* (6634), 815−820.

https://doi.org/10.1021/acs.est.3c05142
Environ. Sci. Technol. 2024, 58, 2413−2422